SRTM C-Band and ICESat Laser Altimetry Elevation Comparisons as a Function of Tree Cover and Relief

Claudia C. Carabajal and David J. Harding

Abstract

The Geoscience Laser Altimeter System (GLAS) instrument onboard the Ice, Cloud, and land Elevation Satellite (ICESat) provides a globally distributed elevation data set that is well-suited to independently evaluate the accuracy of digital elevation models (DEMs), such as those produced by the Shuttle Radar Topography Mission (SRTM). We document elevation differences between SRTM C-band 1 and 3 arcsecond resolution DEMs and ICESat 1064 nm altimeter channel elevation data acquired in an areas of variable topography and vegetation cover in the South American Amazon Basin, Asian Tibetan Plateau – Himalayan Mountains, East Africa, western Australia, and the western United States. GLAS received waveforms enable the estimation of SRTM radar phase center elevation biases and variability with respect to the highest (canopy top where vegetated), centroid (distance-weighted average), and lowest (ground) elevations detected within ICESat laser footprints. Distributions of ICESat minus SRTM elevation differences are quantified as a function of waveform extent (a measure of within-footprint relief), SRTM roughness (standard deviation of a 3 × 3 array of elevation posts), and percent tree cover as reported in the Vegetation Continuous Field product derived from Moderate Resolution Imaging Spectrometer (MODIS) data. SRTM roughness is linearly correlated with waveform extent for areas where percent tree cover is low. The SRTM phase center elevation is usually located between the ICESat highest and lowest elevations, and on average is closely correlated with the ICESat centroid. In areas of low relief and sparse tree cover, the mean of ICESat centroid minus SRTM phase center elevation differences for the five regions examined vary between −3.9 and 1.0 m, and the corresponding standard deviations are between 3.0 and 3.7 m. With increasing SRTM roughness and/or tree cover, the SRTM elevation remains essentially unbiased with respect to the ICESat centroid but the standard deviations of the differences increase to between 20 and 34 m, depending on the region. For the Australia, Amazon, Africa, United States, and Asia regions, including all tree cover and roughness conditions, 90 percent of the SRTM elevations are within 6.9, 11.5, 12.1, 16.8, and 37.1 m of the ICESat centroid, respectively. In vegetated areas, the SRTM elevation on average is located approximately 40 percent of the distance from the canopy top to the ground. The variability of this result increases significantly with increasing SRTM roughness. The results are generally consistent for the five regions examined, providing a method to estimate for any location the correspondence between SRTM elevations and highest, average, and lowest elevations using the globally-available MODIS-derived estimate of tree cover and the measure of SRTM roughness.

Introduction

Understanding the quality of land topography data sets, as represented in Digital Elevation Models (DEMs), is crucial to their appropriate use in land process studies, as inputs to models dependent on topography and for detection of topographic changes obtained from comparison of DEMs acquired at different times. The Ice, Cloud and land Elevation Satellite (ICESat) provides a globally-distributed elevation data set of very high accuracy that is well suited for independent estimation of the vertical accuracy of continental DEMs. The Shuttle Radar Topography Mission (SRTM), using a dual-antennae, single-pass Interferometric Synthetic Aperture Radar (INSAR) operating at a wavelength of 5.6 cm (C-band), has produced the most accurate near-global DEM covering most land and adjacent near-shore ocean areas between latitudes 56° south and 60° north (Farr and Kobrick, 2000; Rabus *et al.*, 2003). The SRTM DEM is produced with a spatial sampling of 1 arcsecond (approximately 30 m) and the elevation reported is the C-band phase center produced by radar scattering from vegetation, buildings, structures, and the ground surface. For the United States and Territories, the C-band DEM has been released with a grid spacing of 1 arcsecond. Elsewhere in the world the data is distributed with a 3 arcsecond grid spacing.

ICESat, a NASA Earth Observing System mission launched in January 2003, carries the Geoscience Laser Altimeter System (GLAS) which has altimetry and atmospheric lidar channels operating at 1064 nm (near-infrared) and 532 nm (green), respectively. GLAS measures the travel time of laser pulses reflected from approximately 65 m diameter footprints spaced 172 m apart along profiles and the orientation of the laser vector. Combining the altimetry channel ranging distance, derived from the travel time, and the laser pulse orientation with spacecraft position, established by precision orbit determination, yields the horizontal and vertical position of the laser footprint in an Earth-fixed coordinate

Claudia C. Carabajal is with NVI, Inc. at the NASA Goddard Space Flight Center – Code 697 – Space Geodesy Laboratory, Greenbelt, MD 20771 (Claudia@bowie.gsfc.nasa.gov).

David J. Harding is at the NASA Goddard Space Flight Center – Code 698 – Planetary Geodynamics Laboratory.

Photogrammetric Engineering & Remote Sensing
Vol. 72, No. 3, March 2006, pp. 287–298.

0099-1112/06/7203–0287/$3.00/0

frame. Zwally *et al.* (2002) and Schutz *et al.* (2005) describe mission details and data products and their accuracies.

Altimeter channel waveforms record the 1064 nm energy of the transmit pulse and received echo (Plate 1) sampled at 1 Gigahertz (1 nsec, equivalent to 15 cm one-way travel). Laser footprint diameter varies with laser operating conditions. For the laser operations period used here, the footprint was slightly elliptical, averaging 46.3 ± 0.7 m and 54.7 ± 0.2 m for the minor and major axis, respectively (M. Sirota, personal communication, 2005). The received waveform represents the height distribution of illuminated surfaces within the laser footprint. Waveform attributes and derived products are described in Harding and Carabajal (2005). In this work, we use ICESat products referred to as "alternate" products that are appropriate for complex land surfaces, as opposed to the "standard" products intended for use with waveforms from smooth ice sheet surfaces. The alternate products include a measure of signal start and end, defined as the first and last crossings of a low threshold, and the signal centroid, a distance-weighted average corresponding to the center of gravity of the signal between start and end (Plate 1). Elevations of the highest detected, average, and lowest detected elevations within the laser footprint are derived from signal start, centroid, and end, respectively. The alternate products also include a representation of the location of peaks between signal start and end (Plate 1), modeled as the sum of up to six discrete Gaussian distributions (Brenner *et al.*, 2003).

Waveform extent corresponds to the distance between the alternate signal start and end. Because the width of the transmit pulse waveform at the threshold level is approximately 2 m, received waveforms reflected from non-vegetated flat surfaces yield a nominal waveform extent of 2 m. Ranging precision is not equivalent to the waveform extent, but rather is approximately 3 cm for flat surfaces achieved by measuring the time between centroids of the transmit and receive waveforms (Abshire *et al.*, 2005; Fricker *et al.*, 2005; Schutz *et al.*, 2005). With increasing topographic relief, the waveform extent increases. In vegetated areas, signal start corresponds to the upper canopy surface where plant area is dense enough to yield a return signal above the threshold level. Signal end corresponds to the lowest detected ground elevation, where sufficient laser energy is reflected from the ground through gaps in the vegetation canopy. For returns from vegetated, low relief terrain, where the received waveform has separate returns from the canopy and ground (as in Plate 1), the amplitude of the canopy return in comparison to the ground return is a measure of canopy closure (nadir-projected plant area compared to total area). For this work, we compute a waveform centroid relative height (WCRH) that is a measure of the position of the centroid with respect to the signal start and end equal to (centroid elevation – signal end elevation)/(signal start elevation – signal end elevation). WCRH approaches values of one and zero when the centroid is close to signal start and end, respectively. Where the canopy and ground returns are

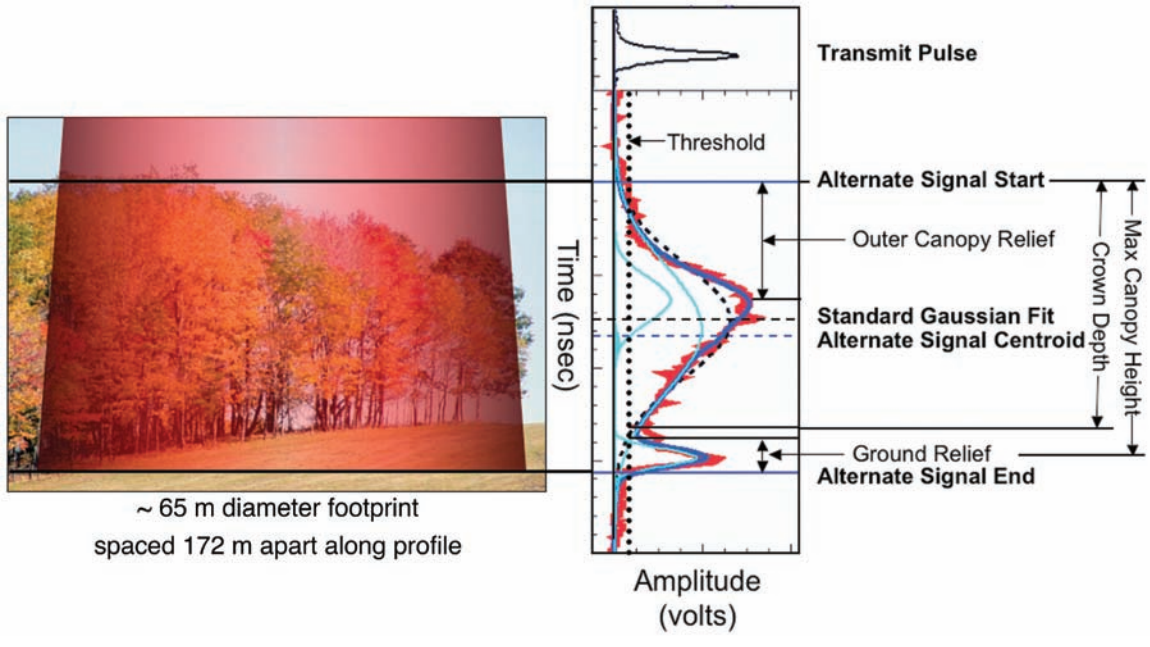

Plate 1. Representative ICESat 1064 nm transmit pulse (upper right, black) and received waveforms (right, red) (modified from Harding and Carabajal, 2005). The transmit pulse waveform is approximately Gaussian in its distribution and 6.0 ns (~1 m) wide at half the maximum amplitude. The received waveform is typical of returns from tree cover on flat ground. The alternate threshold (dotted line), alternate signal start and end (horizontal blue lines) and centroid (horizontal dashed blue line) are used to derive highest, lowest, and centroid ICESat elevations. The "standard" fit (black dashed line), "alternate" fits (cyan), and alternate model fit from the sum of the alternate Gaussians (thick blue line) that result from waveform processing are also shown. Time axis is shown with 10 ns ticks. The received and transmit pulse waveform amplitudes are scaled separately. Crown depth is the distance from the canopy top to the lowest major branch. Maximum canopy height is the distance from the canopy top to the centroid of the ground return. The tree cover depicted is illustrative; it does not correspond to the location of the waveform.

separate, high and low values of WCRH correspond to high and low canopy closure, respectively.

ICESat's capability to measure the vertical distribution of vegetation and the underlying ground provides a means to assess the SRTM elevation results, in particular the amount of C-band microwave penetration into vegetation canopies and elevation biases with respect to the ground surface in vegetated landscapes. Plate 2 illustrates the relationship between SRTM and ICESat elevation profiles for highest, centroid and lowest ICESat-detected surfaces along a profile segment across a largely vegetated region of the Amazon basin, acquired on 07 November 2004. Where tree cover is present, the SRTM elevation is biased upward above the ground into the canopy and corresponds closely to the ICESat centroid. The depth of C-band penetration into the canopy varies along the length of the profile. In a previous study (Carabajal and Harding, 2005), we described a methodology for evaluating SRTM elevation data as a function of vegetation cover and relief using ICESat, and presented results for SRTM 1 arc second resolution data in a region of the Western United States (WUS). In this study, we report elevation differences between SRTM and ICESat waveform highest, centroid, and lowest elevations for regions in South America, Asia, Africa, and Australia, shown in Plate 3, where SRTM products were distributed with 3 arcsecond resolution. Using a similar approach to Carabajal and Harding (2005), we establish empirical relationships between elevations derived from the ICESat received waveforms and SRTM C-band radar phase-center elevations as a function of geographic region, percent tree cover, and relief. Previously reported results for the WUS are included here for comparison.

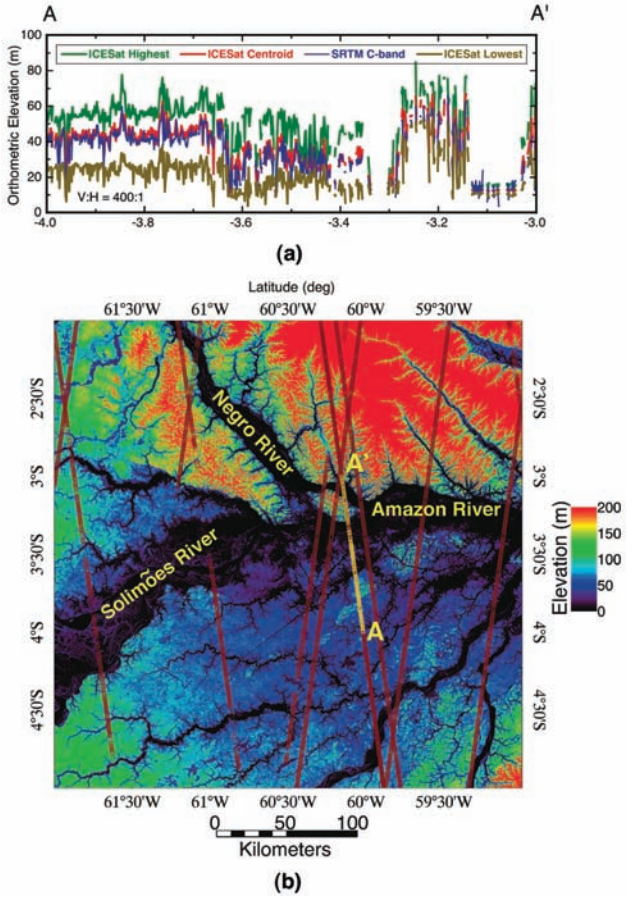

Plate 2. (a) ICESat highest (green), centroid (red) and lowest (brown) and SRTM C-band elevations, bilinearly interpolated to the ICESat footprint locations, along a profile segment (A-A′, Track 433, Laser 3a period, 07 November 2004) across the Amazon River. Gaps in the profiles correspond to voids in the SRTM data or excluded ICESat data inferred to be from cloud tops or to be surface returns distorted by receiver saturation; (b) color-coded 90 m resolution SRTM C-band elevation data for the confluence of the Negro and Solimões Rivers, forming the Amazon River, ICESat Laser 3a period ground tracks (brown), and the A-A′ profile segment (yellow). Gaps in the ICESat tracks correspond to areas of dense cloud cover.

Data Used

SRTM Data

SRTM was flown aboard NASA Space Shuttle Endeavour (STS-99) on 11–22 February 2000 in a 233 km altitude orbit at an inclination of 57°. It was a joint mission conducted by NASA and the National Geospatial-Intelligence Agency (NGA). The SRTM instrument consisted of a C- and X-band INSAR with transmit and receive antennae housed in the shuttle cargo bay and a second receive antenna deployed on a 60 m boom. The C-band component was provided by the Jet Propulsion Laboratory (JPL) and the X-band component by the German and Italian space agencies (Farr and Kobrick, 2000; Rabus *et al.*, 2003). SRTM C-band data was collected in a ScanSAR mode, with a swath width of 225 km to cover the globe with minimal gaps. The mission specification for absolute horizontal and vertical accuracy of the C-band radar phase center is 20 m (circular error at 90 percent confidence) and 16 m (linear error at 90 percent confidence), respectively. The SRTM data used in this study is the "unfinished, research-grade" product processed at JPL and distributed in 1° × 1° cells by the United States Geological Survey EROS Data Center. The globally distributed, research-grade 3 arcsecond data set was produced by spatially averaging the 1 arcsecond data.

Details of the SRTM mission configuration, data processing, and error estimates can be found in Farr and Kobrick (2000), and Rabus *et al.* (2003). A full report of the SRTM errors was done by JPL (Rodriguez *et al.*, 2005). Error contributors to the data stem from subsystems of the space shuttle and instrument characteristics. Data used for system calibration and accuracy assessment activities included kinematic GPS tracks in North America, South America, Australia, Europe, and Africa, static calibrations using corner reflector arrays in the United States and Australia, short and long ocean data takes, ocean ground control points (GCPs) from crossovers, other NGA and JPL on-land (GCPs), DEM "Chip" data generated by NGA from optical imagery, and radar altimeter-derived GCPs obtained by JPL. Random errors are the result of the number of overlapping ScanSAR swaths used in construction of the DEM and the quality of the inteferograms, which is mainly dependent on the strength of the phase coherence. The horizontal accuracy is driven by errors in antenna position knowledge and interferometric phase correlation, which translate into errors in the slant range.

Overall, the horizontal accuracy was found to be better than the requirement, as verified by correlation of ascending and descending orbits. Vertical errors in the SRTM data derive from several sources: instrument errors (thermally

induced noise of ±4 m at 30 m scales, and thermal drifts of <10 m at 8,000 km scales), residual Precision Attitude Determination (PAD) errors (±10 m at 700 km scales from maneuvers and ±1 m from residual oscillations at 50 km scales, ±0.5 m from motion aliasing at 8 km scales), and residual mosaicing errors. Nevertheless, the absolute vertical accuracy was also found to be better than the mission requirement. Estimates of absolute height errors from kinematic GCPs (Rodriguez *et al.*, 2005) show means of −0.7 ± 3.7 (6.6 m, 90 percent) in Eurasia, 0.1 ± 4.0 m (6.5 m, 90 percent) in North America, 1.3 ± 3.8 m (6.0 m, 90 percent) in Africa, 1.7 ± 4.1 m (7.5 m, 90 percent) in South America, and 1.8 ± 3.5 (6.0 m, 90 percent) in Australia. These land elevation accuracy validations were conducted in vegetation free areas, where the C-band radar phase center elevation should correspond to the ground surface and direct comparison between ground truth elevations and SRTM is straightforward. In vegetated landscapes, where the C-band radar phase center is located within the vegetation canopy, the accuracy validation is more complex. Furthermore, the kinematic GPS surveys are restricted to roads that generally sample flat to low slope terrain. Comparisons between SRTM and X-Band GEOSAR derived DEMs collected in Santa Barbara County, California, during 2001 and 2002 were done by JPL (Rodriguez *et al.*, 2005). The GEOSAR DEM's relative height accuracy is 1.0 m (1 sigma), and 2.5 m absolute, averaged over the 10 km swath with 5 m postings, in this area largely comprised by agricultural fields and vineyards. SRTM to GEOSAR comparisons show differences of 0.54 ± 3.32 m., with 50 percent of the differences between −0.9 m and 2.1 m, and 90 percent between −4.5 m and 5.8 m. It was observed that neither the GEOSAR X-Band nor the SRTM C-Band data measure the true ground surface, and heights differ significantly (by up to 15 m), in the presence of vegetation cover.

ICESat Data

The ICESat data used in this study were acquired in October-November 2004, referred to as the "Laser 3a operation period." Elevation products used here are those provided in the ICESat GLA14 (land) product distributed as Release 22, which includes corrections applied to the laser pointing orientation (Laser Reference Sensor (LRS) corrections applied to the Instrument Star Tracker (IST) data and the IST field-of-view (FOV) distortion), but does not include ocean scan nor round the world scan pointing corrections that account for orbital and longer-period, thermally-induced pointing errors (Schutz *et al.*, 2005). At the time of this analysis, fully calibrated data were only available from the September through December 2003 Laser 2a operation period. However, these data were acquired with a maximum waveform height range (extent) of 82 m that caused truncation of the upper part of waveforms where vegetation cover is tall and/or slopes are steep (Harding and Carabajal, 2005). Using a waveform compression scheme, the Laser 3a period data was acquired with an extent of 150 m that minimized waveform truncation making it more suitable for assessment of the SRTM DEMs. Other ICESat operation periods were collected during times of northern hemisphere "leaf-off" foliage conditions (March 2003, 2004, and 2005), comparable to the time frame when SRTM data were collected. However, at the time of this analysis these data had less complete laser pointing calibration corrections applied and were thus less accurate than the period used.

Pointing errors remaining in the ICESat data translate into horizontal and vertical (elevation) geolocation errors. An estimate of the Laser 3a, Release 22 pointing error based on integrated residual analysis of ocean returns (Luthcke *et al.*, 2000) yields a mean and standard deviation of 0.84 ± 2.5 arcseconds corresponding to a horizontal geolocation error of 2.4 ± 7.3 m (Luthcke, personal communication, 2005). The magnitude of the elevation error depends on the incidence angle between the laser vector and the surface normal. The vertical error is 0.04 ± 0.13 m per degree incidence angle for Laser 3a, Release 22. The error can be negative or positive depending on the slope of the surface and the azimuth of the pointing error. The laser vector points at a nominal 0.3° off-nadir angle, avoiding very intense specular reflections from smooth water. This translates into a 0.01 ± 0.04 m vertical error for flat surfaces. For surface slopes of 10° the mean ± three sigma pointing error translates into an elevation error that varies between ±4 m.

The regions selected for comparison of SRTM and ICESat elevations include a variety of topographic relief and vegetation cover types (Plate 3). The WUS region showed a wide range of vegetation cover and relief. The Amazon was used as an example of a region with dense vegetation cover and low relief, while the region in Australia was chosen as representative of low relief and sparse vegetation cover. The area in Africa exhibited moderate relief and vegetation cover, while the region in Asia showed sparse vegetation cover, but a combination of low relief in the Tibetan Plateau, and high relief Himalayan Mountains to the south.

For comparison to SRTM, we converted ICESat data to the same geodetic reference frame (WGS84; NGA, 1994). Ellipsoidal elevations were converted into orthometric elevations by applying the EGM96 geoid value (Lemoine *et al.*, 1998) interpolated to the footprint locations, after converting ICESat elevations to the WGS84 ellipsoid (Carabajal and Harding, 2005). At the latitude and longitude location of each ICESat footprint, the corresponding SRTM radar phase center elevation was computed using bilinear interpolation. A measure of SRTM elevation variability was also computed for an area surrounding the ICESat footprint using the standard deviation of the SRTM elevations reported for the 3 by 3 array of posts (approximately 90 m by 90 m for the WUS, and approximately 270 m by 270 m elsewhere) centered at the ICESat geolocation point. This value, which we refer to as SRTM roughness, is due to the combined effects of topographic relief, SRTM measurement noise (i.e., post-to-post relative elevation error), and where vegetated, variable C-band microwave penetration into the vegetation cover.

Data voids in either the SRTM or ICESat data locally precluded comparison of elevations. In areas of high relief, were radar shadowing occurs, or in areas where coherence is lost, there are voids in the SRTM elevation data. For the ICESat data, returns from the Earth's surface are obtained through thin cloud cover. However, thick cloud cover prevents the laser pulse energy from reaching the ground and either no return is detected or the return, and reported elevation, is for the cloud top. For all regions except that in Asia, the tails of the distributions of ICESat centroid minus SRTM elevation differences decrease to near zero beyond ±20 m to ±50 m. Outlier occurrences where the ICESat elevation is more than 100 m above the SRTM DEM are associated with laser returns from cloud tops, and have been excluded from this analysis using a ±100 m ICESat centroid to SRTM elevation difference edit. There are instances where ICESat returns from very low-lying clouds or fog are included in the analysis. In the Asian region, the steep Himalayan Mountain slopes causes a broader distribution of ICESat to SRTM elevation differences, and the ±100 m editing excludes a small fraction of valid differences.

In order to exclude ICESat data with potential error sources that could degrade its accuracy, we have also edited the data to remove truncated and saturated returns. Waveform truncation was identified if the waveforms extent

exceeded 148.0 m (waveforms only sampled up to 150 m). Where the return energy exceeds the linear response range of the GLAS receiver, the waveforms become saturated and thus distorted (Abshire *et al.*, 2005). The distortion introduces a range delay that depends on the degree of saturation (a function of the receiver gain and signal strength; Xiaoli Sun, personal communication, 2005), causing a low elevation bias of centimeters (for slight saturation) to meters (for severe saturation). For this analysis, waveforms with smoothed return amplitudes greater or equal to 1.4 Volts were identified as saturated and not included.

We have not excluded ICESat data that potentially have range delays as a result of atmospheric forward scattering (Duda *et al.*, 2001; Spinhirne *et al.*, 2005). The magnitude of this range delay depends on the cloud and aerosol optical depth, particle size, and altitude, and can introduce a too-low elevation bias of centimeters to meters. A forward scattering flag and correction is being implemented by the ICESat project for distribution with the data, and it use will be incorporated in successive analyses of the SRTM DEMs.

No editing of the ICESat data was done based on off-nadir pointing of the laser beam. Off-nadir pointing introduces elevation errors that are a function of the angle with which the surface is intercepted by the laser beam. For selected targets, the ICESat spacecraft is pointed up to 5° off-nadir; however, most of the data used were acquired at the nominal near-nadir pointing orientation.

MODIS Data

To investigate the effects of vegetation cover on SRTM elevation biases, we used the areal proportional estimate of woody vegetation, provided in the 500 m resolution Vegetation Continuous Fields (VCF) product from the Moderate Resolution Imaging Spectroradiometer (MODIS) (Hansen *et al.*, 2003). The woody vegetation estimate is referred to as the percent tree cover layer. VCF woody vegetation, herbaceous vegetation, and bare cover estimates were developed from cloud-corrected, monthly composites of MODIS surface reflectance using global training data (representative known pixels that describe the spectral range of every class) derived using high-resolution imagery by Hansen *et al.*, 2003. The sum of the three cover layers for each 500 m pixel equals 100 percent. These training data applied to MODIS phenological metrics are used with a regression tree to derive percent cover globally. For this analysis we used the percent tree cover value for the pixel in which the ICESat footprint is located, and grouped the data in five categories (0 percent to 20 percent, 20 percent to 40 percent, 40 percent to 60 percent, 60 percent to 80 percent, and 80 and 100 percent tree cover).

Results

Plate 3 shows the geographic distribution of color-coded ICESat centroid minus SRTM elevation differences along Laser 3a profiles for the Amazon Basin and Asia. Gaps in the differences profiles are due to cloud cover or absence of SRTM data (voids). Larger elevation differences, either positive or negative, are associated with areas of greater topographic relief and/or forest cover. Histograms of elevation differences for the ICESat highest, centroid, and lowest elevations with respect to SRTM are shown in Plate 4, and summary statistics for all regions are reported in Table 1. The centroid elevation minus SRTM histogram for the Amazon (red) is symmetric and strongly peaked, with small mean difference of −1.94 m, a median of −1.43 m, and a standard deviation of 7.30 m. The difference histograms for the highest and lowest elevations are also strongly peaked but are somewhat broader than the centroid difference distribution and are offset to mean differences of 14.46 m and −22.35 m, respectively. The distribution for lowest elevation differences is bimodal, with a smaller population peaked at −4.40 m related to returns from non-vegetated areas of low relief. Isolated artifacts in the ICESat lowest elevation profile extend approximately 10 to 15 m below the ground surface (e.g. Plate 2) which contribute to the negative tails in the lowest minus SRTM distributions. These artifacts are caused by anomalously high signal occurring after the return from the ground, possibly due to elevated noise that sometimes follows strong surface returns or due to range-delayed tails caused by forward scattering during transmission through low clouds or the canopy itself. The difference distributions for the region in Asia each consist of two components, with narrow peaks near zero due to returns from the low-relief, non-vegetated Tibetan Plateau and broad positive and negative tails due to returns from the high-relief Himalayan Mountains. In contrast to the Amazon, the centroid mean and median elevation differences are slightly positive (1.12 and 1.01 m, respectively).

TABLE 1. STATISTICS FOR ICESat HIGHEST, CENTROID, AND LOWEST ELEVATIONS MINUS SRTM ELEVATIONS FOR THE FIVE REGIONS STUDIED, INCLUDING THE 90 PERCENT FREQUENCY OF OCCURRENCE (90 PERCENT OF THE ABSOLUTE VALUE OF THE DIFFERENCES ARE EQUAL TO OR LESS THAN THIS VALUE)

Region	ICESat Elevation	Mean (m)	Median (m)	STD (m)	90 percent (m)
Western US	Highest	16.52	15.33	13.66	31.38
N = 28218	Centroid	−3.99	−2.17	9.53	16.78
	Lowest	−21.75	−19.22	16.36	44.37
Amazon	Highest	14.46	13.89	10.01	24.46
N = 255646	Centroid	−1.94	−1.43	7.30	11.45
	Lowest	−22.35	−22.81	11.79	35.99
Africa	Highest	5.14	4.35	11.07	15.71
N = 25004	Centroid	−3.63	−3.91	9.60	12.06
	Lowest	−9.84	−8.89	10.69	19.05
Asia	Highest	13.76	5.81	24.87	47.83
N = 32113	Centroid	1.12	1.01	21.69	37.14
	Lowest	−11.06	−3.74	24.88	46.27
Australia	Highest	−0.11	−0.41	4.24	6.14
N = 29174	Centroid	−2.79	−2.80	3.91	6.86
	Lowest	−5.28	−5.06	3.92	9.06

For the WUS, centroid mean and median differences are negative (−3.99 m and −2.17 m), and distributions for differences with respect to highest and lowest are bimodal and less uniform, since the area comprises a wide range of topographic relief and vegetation cover. Similar results are obtained for the Africa and Australia regions, where centroid differences are negative by several meters and nearly all the SRTM elevations occur below the ICESat highest elevation and above the ICESat lowest elevation. Tighter, single-peaked distributions of differences, and thus, lower standard deviations are observed for Africa and Australia due to the lower relief and sparser vegetation cover.

For all five regions, the means, medians, and peaks of the centroid minus SRTM elevation differences are between −3.99 and 1.12 m, with all but Asia being negative. In addition, for all regions the SRTM elevation on average is located further above the ICESat lowest elevation than it is below the highest elevation (i.e., SRTM elevation is closer to the highest elevation). For all regions the standard deviation of the centroid differences is smaller than that of the highest and lowest elevation differences, and are all less than 10 m with the exception of Asia where the steep Himalayan topography causes larger differences.

The relationship between ICESat waveform extent, which includes the combined effects of terrain relief (slope and

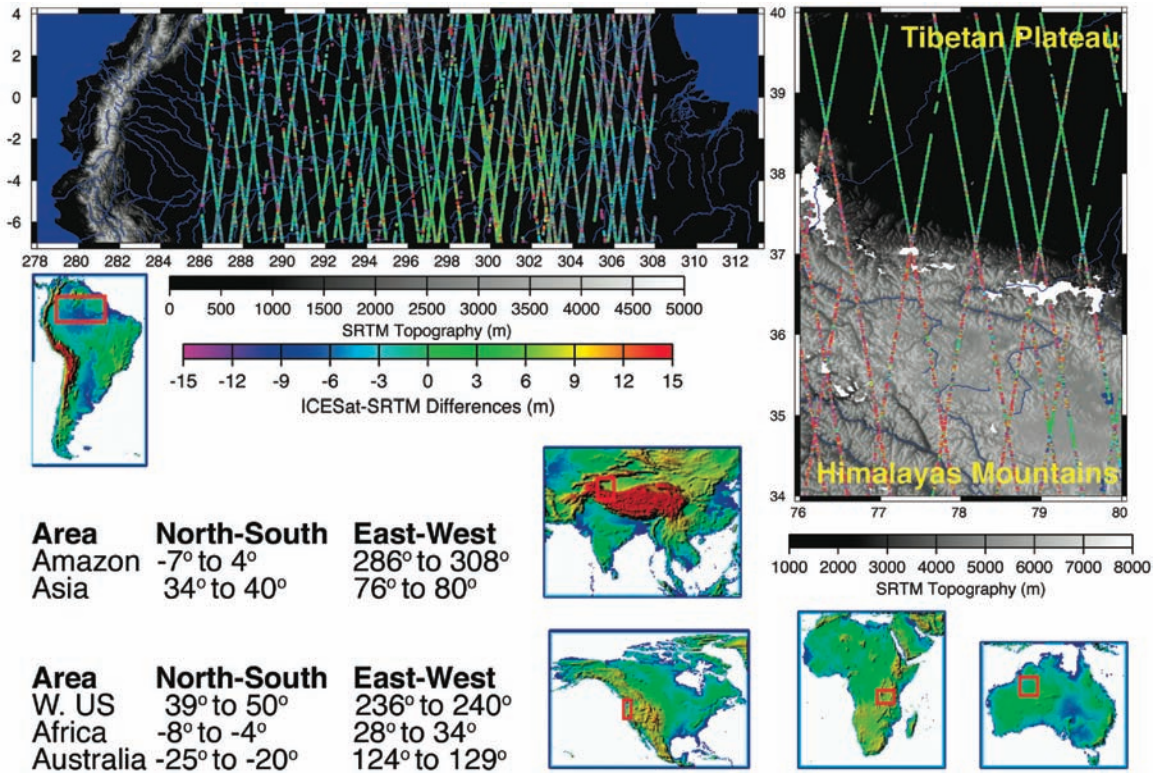

Plate 3. ICESat Laser 3a operation period profiles (October and November 2004) for the study areas in the Amazon Basin and Asia superimposed on SRTM topography, and the locations of the five regions evaluated (red boxes on inset maps). The magnitude of the differences between ICESat's centroid and SRTM elevations are shown by the color bar. Elevation differences larger than ±15 m are shown as magenta and orange.

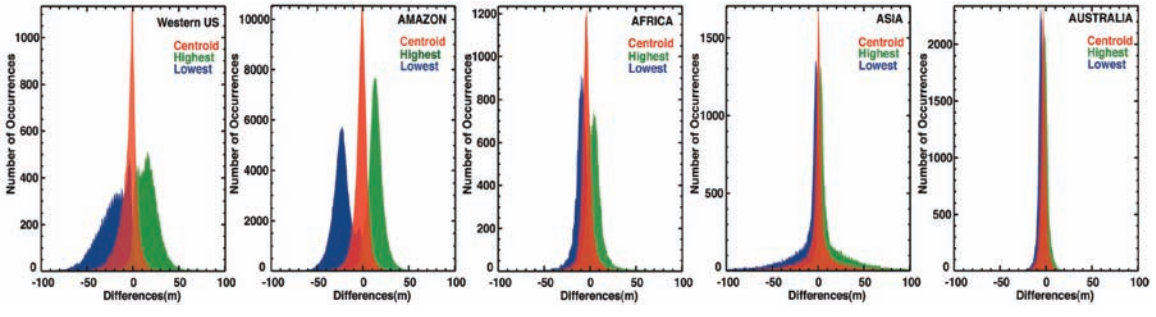

Plate 4. Overlapping histograms of differences between ICESat highest (green), centroid (red) and lowest (blue) detected elevations minus SRTM elevations for the regions in Western U.S., South America (Amazon Basin), Africa, Asia, and Australia. Statistics for the distributions are shown in Table 1.

roughness) and vegetation cover, and SRTM roughness is shown in Plate 5. Regression lines show similar slopes near one for all non-U.S. regions where the SRTM grid spacing is 90 m, and a steeper regression slope in the WUS due to the 30 m grid sampling, yielding lower SRTM roughness values. For the region in Asia, where waveform extent is primarily related to relief rather than vegetation effects, the data are more uniformly centered about the regression line (lower sigma, higher R^2), with increasing scatter for larger relief. This relationship indicates that the SRTM roughness parameter is an estimate of topographic relief in non-vegetated areas. The approximately 6 m *Y*-axis intercept may be due to measurement noise in the SRTM elevations.

The Amazon basin relationship, where topographic relief is low and vegetation cover effects dominate, is more complex. A data cluster with both low waveform extent and SRTM roughness, and WCRH values near 0.5, corresponds to areas of sparse and/or low stature vegetation. The cluster with waveform extents from 20 to 80 m and SRTM roughness varying from 0 to 50 m, and usually high values of WCRH

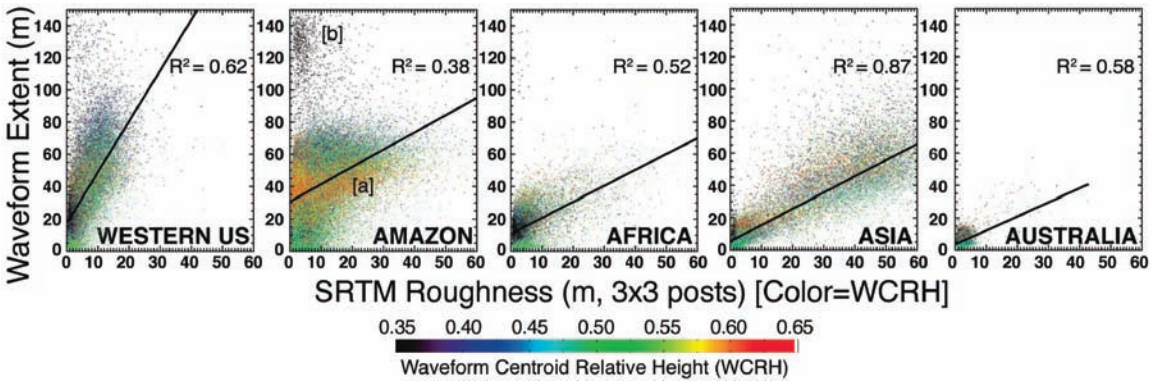

Plate 5. Relationship between ICESat waveform extent and SRTM roughness (standard deviation of SRTM elevations within a 3 by 3 posts region equal to 90 m by 90 m for the U.S. and 270 m by 270 m elsewhere). Regression lines to the data are shown in black. Corresponding equations showing slope and intercept values and the standard deviation of the fit are shown in Table 2. Data are color-coded by WCRH.

TABLE 2. REGRESSION RELATIONSHIPS BETWEEN ICESat WAVEFORM EXTENT AND SRTM RELIEF AS ESTIMATED FROM THE STANDARD DEVIATION OF THE ELEVATIONS WITHIN A 3 BY 3 POSTS REGION CENTERED AT THE ICESat FOOTPRINT LOCATION. SCATTER PLOTS SHOWING THESE RELATIONSHIPS ARE SHOWN IN PLATE 5

	ICESat Waveform Extent vs. SRTM Roughness (3 × 3 posts region centered at ICESat'S footprint) Y (m) = Slope * X (m) + Intercept (m)			
Region	Slope	Intercept (m)	Sigma (m)	R^2
Western US	3.17	17.17	17.02	0.62
Amazon	1.07	30.89	13.67	0.38
Africa	0.99	10.52	8.44	0.52
Asia	1.00	5.63	7.10	0.87
Australia	0.87	3.56	1.60	0.58

(Plate 5a), corresponds to areas of dense vegetation cover where the SRTM elevation surface can vary from smooth (with relatively constant elevations due to uniform C-band penetration into the canopy) to more rugged (due to variable penetration). The cluster with very high waveform extent, low SRTM roughness, and very low WCRH (Plate 5b) probably corresponds to areas of low-lying fog where signal start corresponds to weak returns from the fog layer and signal end corresponds to the surface, yielding anomalously large extents and low WCRH values. This effect has been observed in ICESat profiles across fog-filled valleys on ocean islands. The plots for Australia and Africa exhibit a limited distribution of points due to low and moderate relief and vegetation cover, respectively.

The relationships between elevation differences and waveform extent and SRTM roughness for the Amazon and Asia regions are shown in Plate 6. The distributions in Plate 6 indicate that as waveform extent and SRTM roughness increase, the C-band phase center on average is increasingly biased below the ICESat highest elevation and above the ICESat lowest elevation, but is relatively unbiased with respect to the waveform centroid. Scatter with respect to the regression line increases with waveform extent and SRTM roughness, especially so for the steep Himalayan Mountains. Clipping of the distributions observed for the ICESat lowest elevations is due to the ±100 m editing applied to the centroid minus SRTM differences. Clusters observed in Plate 5 related to WCRH also appear in Plate 6. Results for the regions in the Western U.S., Africa, and Australia show similar relationships (Table 3).

The effect of the areal-proportion of tree cover, derived from MODIS, and SRTM roughness on ICESat centroid minus SRTM elevation differences for the WUS were shown in Carabajal and Harding, 2005 (Plate 5 and Table 1). Distributions broaden and become more negatively skewed as the proportion of tree cover increases, and mean differences increase for increased tree cover and roughness. Similar relationships were observed for the regions in this analysis. Elevation difference statistics as a function of VCF tree cover proportion and SRTM roughness classes for the regions in South America and Africa are shown in Plate 7. Water covered areas, which do not have VCF proportions reported, are excluded. For the Amazon, the mean bias is negative for all combinations of tree cover and roughness classes for ICESat centroid minus SRTM elevation differences, becoming steadily more negative as roughness increases but not varying with percent tree cover within a roughness class. The mean biases for the ICESat highest minus SRTM differences are all positive and become larger with increasing roughness, whereas the lowest elevation differences are all negatively biased and become more negative with increasing roughness. For all roughness classes, both the lowest and highest differences have the largest means for the lowest and two highest tree cover classes, whereas the mean differences for the two intermediate tree cover classes are somewhat smaller. The standard deviations within a roughness class are relatively uniform for highest, centroid, and lowest differences, independent of tree cover class, but increase with increasing roughness. For the Amazon, 65 percent of the data is in the ≤5 m roughness category, and 68 percent is in the 80 percent to 100 percent tree cover class. The smallest mean bias and standard deviation (−0.14 m ± 3.65 m), occurs for centroid differences in relatively flat areas (SRTM roughness ≤5 m) with low tree cover (0 to 20 percent), which represent 3 percent of the measurements. For the lowest roughness and highest percent tree cover combination, the mean and standard deviation are −1.23 m ± 5.02 m. For comparable tree cover and roughness class combinations, the ICESat lowest elevations are further below the SRTM elevation, on average, than the highest elevations

TABLE 3. REGRESSION RELATIONSHIPS BETWEEN ICESat MINUS SRTM ELEVATION DIFFERENCES WITH RESPECT TO WAVEFORM EXTENT AND SRTM RELIEF (3 BY 3 POSTS REGION). REGRESSION EQUATIONS FOR THE AMAZON AND ASIAN REGIONS ARE SHOWN IN PLATE 6, INCLUDING VALUES FOR THE SLOPE, INTERCEPT (INT.), AND SIGMA OF THE REGRESSION LINE

		Differences vs. Waveform Extent Y (m) = Slope * X (m) + Int. (m)				Differences vs. SRTM Roughness Y (m) = Slope * X (m) + Int. (m)			
Region	ICESat Elevation	Slope	Int. (m)	Sigma (m)	R^2	Slope	Int. (m)	Sigma (m)	R^2
Western US	Highest	0.39	1.36	6.62	0.77	1.23	7.99	9.35	0.42
N = 28218	Centroid	−0.14	1.53	7.21	−0.36	−0.46	−0.88	7.48	−0.24
	Lowest	−0.61	1.37	6.63	−0.84	−1.99	−8.77	12.22	−0.57
Amazon	Highest	0.36	0.91	5.55	0.68	0.44	11.85	7.45	0.23
N = 255646	Centroid	0.09	1.43	5.77	−0.20	−0.20	−0.82	5.87	−0.14
	Lowest	−0.64	0.91	5.55	−.78	−0.70	−18.65	10.70	−0.32
Africa	Highest	0.56	−3.10	4.83	0.51	0.67	2.41	7.14	0.21
N = 25004	Centroid	−0.001	−3.75	5.03	−0.002	0.10	−4.04	5.02	−0.003
	Lowest	−0.45	−3.11	4.83	−0.46	−0.70	−7.00	6.12	−0.30
Asia	Highest	0.50	1.00	6.94	0.48	0.54	3.53	8.49	0.42
N = 32113	Centroid	−0.004	1.09	6.82	−0.03	−0.018	1.08	6.01	−0.02
	Lowest	−0.49	0.87	6.94	−0.48	−0.52	−1.62	7.84	−0.41
Australia	Highest	0.91	−4.68	2.88	0.42	0.29	−0.66	3.29	0.10
N = 29174	Centroid	0.33	−4.40	2.92	0.10	−0.19	−2.49	2.96	−0.09
	Lowest	−0.10	−4.64	2.88	−0.20	−0.54	−4.33	2.87	−0.27

TABLE 4. MEANS AND STANDARD DEVIATIONS FOR ALL SRTM ROUGHNESS CATEGORIES AND LOW TREE COVER (0 PERCENT TO 20 PERCENT) FOR THE REGION IN ASIA

	ASIA ICESat Centroid − SRTM Elevations		
SRTM Roughness (m) (3 by 3 cells)	Mean (m)	STD (m)	N
≤5	1.03	3.04	15455
5 < Roughness ≤ 10	1.00	7.73	2036
10 < Roughness ≤ 15	0.80	13.28	1104
15 < Roughness ≤ 20	1.13	16.42	1136
>20	1.31	34.16	12272

TABLE 5. MEANS AND STANDARD DEVIATIONS FOR ALL REGIONS STUDIED, FOR LOW TREE COVER (0 PERCENT TO 20 PERCENT) AND LOW SRTM ROUGHNESS (≤5 M)

	All Regions ICESat Centroid − SRTM Elevations (0 percent-20 percent Tree Cover and ≤5 m Roughness)		
Region	Mean (m)	STD (m)	N
Western US	−0.60	3.46	5371
Amazon	−0.14	3.65	7224
Africa	−3.85	3.65	6207
Asia	1.03	3.04	15455
Australia	−2.76	3.37	28723

are above the SRTM elevation, and become more so with increasing tree cover and roughness (Plates 2, 6, and 7).

In most respects, the African region exhibits similar trends to those of the Amazon. However, the mean differences are somewhat more variable, and the standard deviations are larger, especially for higher roughness classes. Also, the trends of lowest and highest mean differences increase consistently from low to high tree cover. The mean and standard deviation for the lowest roughness and percent tree cover class, representing 27 percent of the data, is −3.85 m ± 3.65 m. For the largest represented combination (20 percent to 40 percent tree cover and <5 m relief, comprising 35 percent of the data), the mean and standard deviation are −4.57 m ± 3.88 m.

To investigate the isolated effects of topographic relief on SRTM data accuracy, we present results for the Tibetan Plateau – Himalayan region. Because the MODIS VCF classification indicates no more than 20 percent tree cover (Tables 4 and Plate 8) and SRTM roughness is strongly correlated with ICESat waveform extent (R^2 = 0.87), we infer SRTM roughness is primarily a measure of topographic relief for this region. The centroid difference distribution is very narrow for the lowest roughness region and become increasingly broadened as roughness increases, with standard deviations increasing from 3.04 m to 34.16 m from low (≤5 m) to high (≥20 m) roughness. Centroid mean differences for all roughness classes are similar, close to 1 m.

We summarize the centroid difference results, for all regions studied, for low percent tree cover and all roughness classes in Plate 9. Mean differences are relatively uniform for all roughness classes, but do exhibit more negative means for the WUS and Australian regions for roughness above 15 m, and for the African region for roughness above 20 m. Standard deviations within a roughness class are similar for the five regions, and all regions exhibit increased standard deviations with increasing roughness. Means and standard deviations for centroid differences for the combined low roughness and low percent tree cover category are shown in Table 5. The means range from 1.03 m in Asia to −3.85 m in Africa. The standard deviations are quite similar, ranging from 3.04 m to 3.65 m.

Discussion

The close correspondence between ICESat centroid and SRTM elevations (Plate 2), irrespective of tree cover and SRTM roughness, indicates that C-band radar scatterers and 1064 nm optical reflectors, on average, yield a similar elevation. Thus, the SRTM DEMs can be thought of as representing the average

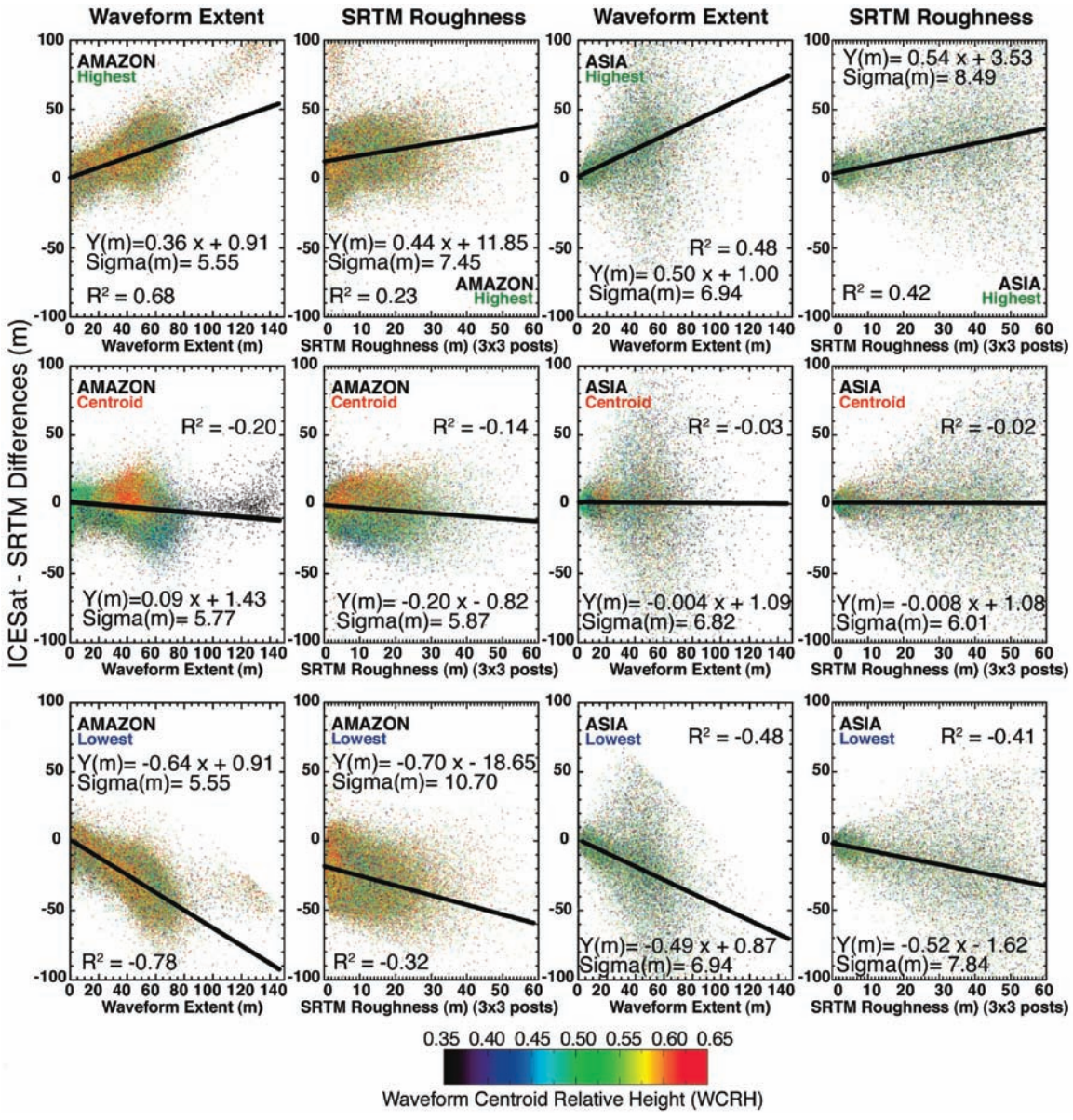

Plate 6. Relationship between ICESat minus SRTM differences for highest, centroid and lowest elevations and ICESat waveform extent and SRTM roughness for the Amazon Basin and Tibetan Plateau – Himalayan regions. Regression lines to the data are shown in black, and corresponding equations show slope and intercept values and the standard deviation of the fit. Data have been color-coded by WCRH.

elevation of nadir-projected surface area. For four of the five regions examined (Table 1), the difference between the ICESat centroid and SRTM is equal to or smaller than the 16 m SRTM vertical accuracy requirement (linear error at 90 percent confidence). For the Asia region, the steep slopes of the Himalayan Mountains cause the differences to be larger. For areas of low relief and sparse tree cover, the means and standard deviations for the ICESat centroid differences versus SRTM are small in all the regions examined, in close agreement with other assessments of SRTM accuracy, indicating that the SRTM data is well within the mission specification for vertical accuracy in this type of terrain. The tendency of the mean centroid differences to become more negative with increasing relief for areas of sparse tree cover (Plate 9) could indicate that the sparse tree cover is preferentially located on steeper slopes causing more upward bias of SRTM relative to the centroid and/or the radar phase center becomes preferentially more sensitive to higher ground surfaces than does ICESat as relief increases. In either case, detection of topographic change by differencing SRTM with other DEMs could introduce an apparent uplift bias as a function of increasing relief, especially when elevation matching of low relief areas is used to adjust vertical datums between disparate DEMs.

In vegetated areas, SRTM elevations with respect to the highest and lowest ICESat elevations as a function of waveform extent (Plates 6 and 7) provide insight into the depth of penetration of C-band microwaves in vegetation canopies. The C-band radar phase center penetrates slightly less than half way into the canopy on average for all the tree

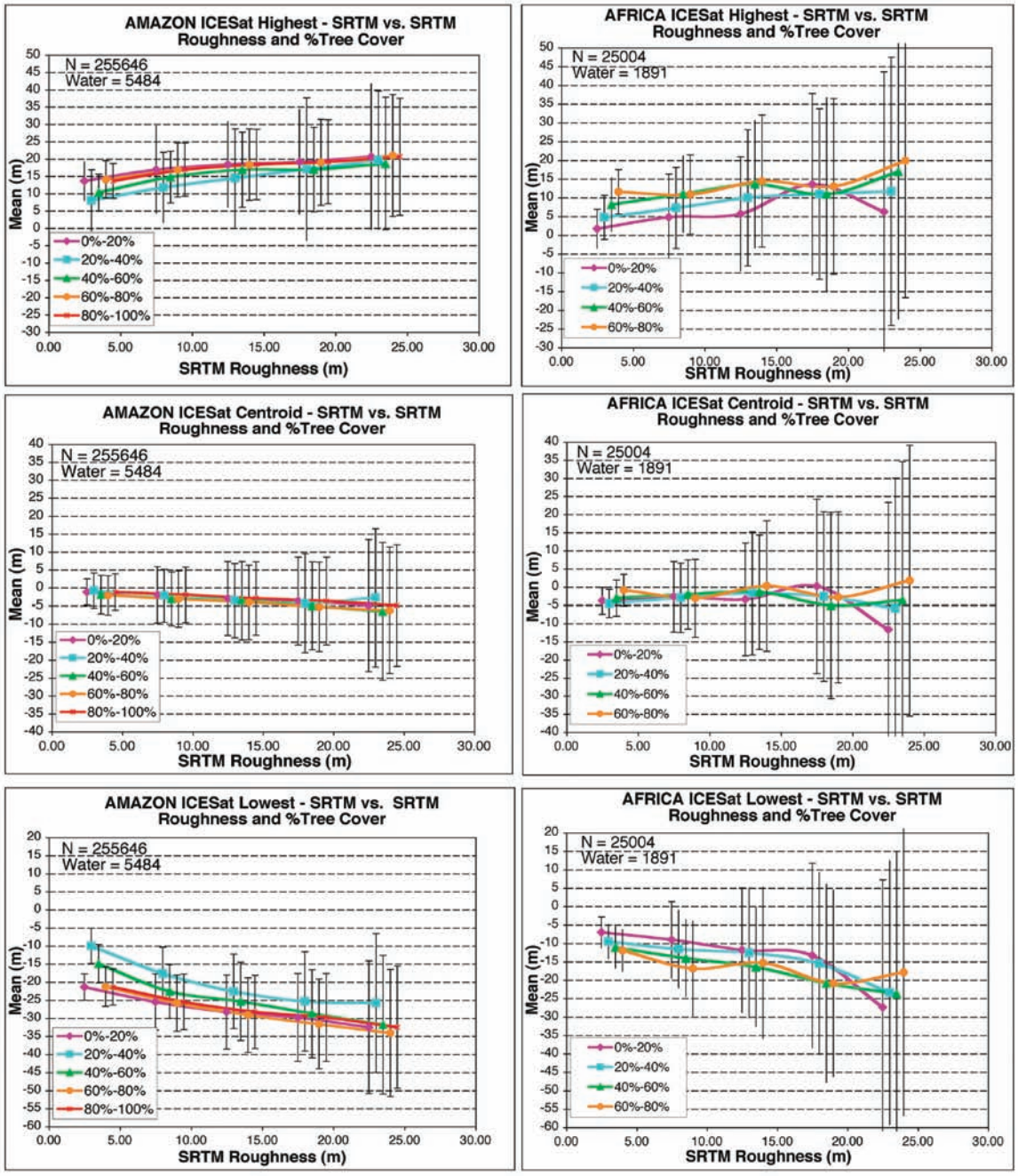

Plate 7. Means and standard deviations for ICESat minus SRTM elevation differences for all classifications of percent tree cover and all SRTM roughness classes considered in this study. The 80 percent to 100 percent tree cover class is poorly represented in Africa (39 footprints for all relief categories), and it has been excluded from the plot. SRTM roughness categories correspond to roughness less than 5 m, 5 to 10 m, 10 to 15 m, 15 to 20 m, and greater than 20 m. Means and standard deviations have been offset for clarity. The number of footprints included in the analysis and those excluded, where classified by the MODIS VCF product as water returns, are shown.

cover classes and the range of waveform extents. With increasing tree cover and waveform extent, the phase center becomes increasingly displaced upward into the canopy as more radar energy is reflected from canopy components and less from the ground, and the variability of the SRTM elevation relative to the highest and lowest surfaces detected by ICESat becomes larger. The increasing upward bias and greater variability make the SRTM elevation an increasingly less reliable measure of ground topography as tree cover increases.

The general consistency of these regional results provides a means to evaluate the applicability of the SRTM elevation data when ground topography data is required. Using the globally-available MODIS VCF tree cover estimates, roughness estimates computed from SRTM, and the relationships presented here, SRTM elevation biases and variability

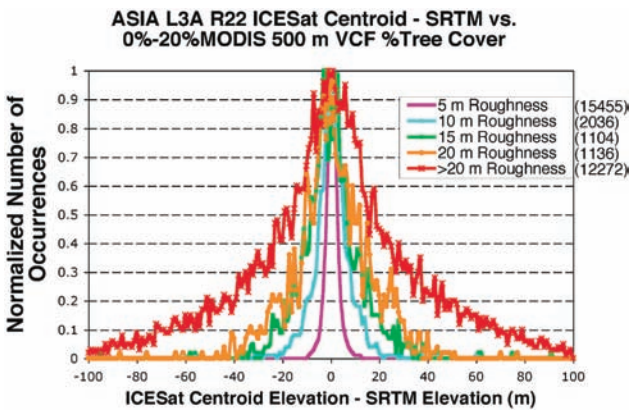

Plate 8. Normalized histograms showing distributions of ICESat centroid minus SRTM elevation differences for the 0 percent to 20 percent tree cover class and all SRTM roughness categories for the region in Asia. Number of returns in each distribution is shown in parenthesis.

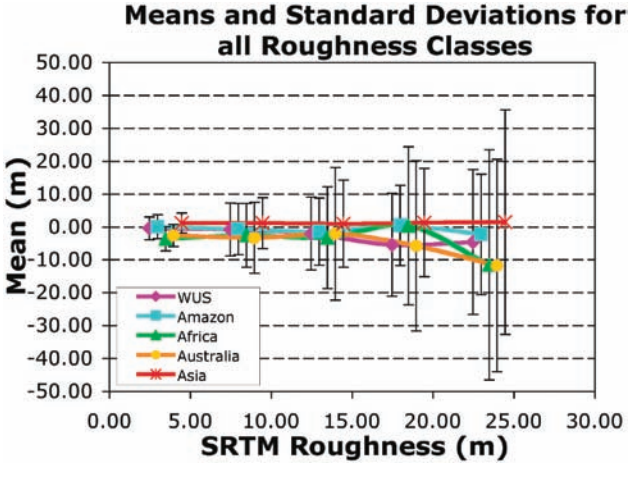

Plate 9. Means and standard deviations for ICESat centroid minus SRTM elevation differences for the 0 percent to 20 percent tree cover class and all SRTM roughness classes, for all regions studied. Roughness categories correspond to roughness less than 5 m, 5 to 10 m, 10 to 15 m, 15 to 20 m, and greater than 20 m. Means and standard deviations have been offset for clarity.

with respect to the ground can be estimated everywhere SRTM data is available. However, as demonstrated by the elevation differences as a function of waveform extent, vegetation canopy height is a principle influence on the distance SRTM is biased above the ground surface. No estimate of vegetation height is currently available globally to incorporate in the characterization of SRTM biases relative to the ground. Potentially, land-cover classifications derived from image sources such as MODIS and Landsat, calibrated using ICESat waveform extent, could be used to estimate vegetation canopy height globally, providing this additional constraint needed to fully evaluate SRTM biases with respect to the ground.

Conclusions

ICESat data's global distribution referenced to a consistent geodetic reference frame, its horizontal and vertical geolocation accuracy, and its ability to resolve the height distribution of elevations within the laser footprint provide a global set of accurate control points. These data enable global assessments of DEM vertical accuracy in areas of various relief and vegetation cover conditions, where calibration and validation data from other techniques may not be available. We have established relationships between SRTM C-band elevations and ICESat waveform-derived highest, centroid, and lowest elevations for regions on five continents as a function of waveform extent, SRTM roughness, and tree cover. SRTM roughness is an estimate of topographic relief in areas of sparse tree cover. For areas of low relief and sparse tree cover, SRTM C-band phase center elevations, in a mean sense, are between 3.9 m below and 1.0 m above the ICESat waveform centroid and the variability of the differences is small (standard deviations between 3.0 and 3.7 m). These estimates of SRTM accuracy are consistent with other estimates for low relief and sparsely vegetated areas, indicating that the errors are well below the 16 m at 90 percent confidence vertical accuracy specification for the SRTM mission for this type of terrain.

As SRTM roughness and/or tree cover increase, SRTM elevations remain essentially unbiased with respect to the ICESat centroid, although in some regions SRTM becomes biased upward by up to 10 m with respect to the centroid in areas of high SRTM roughness. For the five regions in Australia, Amazon, Africa, United States, and Asia, including all tree cover and roughness conditions, 90 percent of the SRTM elevations are within 6.9, 11.5, 12.1, 16.8, and 37.1 m, respectively of the ICESat centroid. The latter large value is due to the steep Himalayan Mountain area included in the Asia region. The standard deviation of ICESat minus SRTM elevation differences is relatively constant as a function of percent tree cover within SRTM roughness class, but increase substantially with increasing roughness (from approximately 3 m to as much as 20 to 34 m, depending on the region). The SRTM elevations are for the most part located between the ICESat detected highest and lowest elevations. In vegetated areas the SRTM elevation, on average, is located about 40 percent of the way from the canopy top to the ground, with the variability of this result increasing with SRTM roughness. Based on these results, which are generally consistent for all five regions examined, the relationship of SRTM elevations to highest, average, and lowest elevations can be estimated at the SRTM DEM cell-scale using globally-available MODIS-derived estimates of percent tree cover and SRTM roughness. These insights into the characteristics of the SRTM elevation data will improve its utilization in the wide variety of scientific investigations and applications programs that require accurate representations of the Earth's topography.

Acknowledgments

This research was supported by NASA's ICESat Project and Solid Earth and Natural Hazards Program (RTOP 622-74-10). We thank the ICESat Science Project and the National Snow and Ice Data Center for distribution of the ICESat data (see **http://icesat.gsfc.nasa.gov** and **http://nsidc.org/data/icesat/**), the ICESat Science Investigator-led Processing System and Science Computing Facility staff, especially K. Barbieri and J. Guerber, for providing valuable assistance, and S. Luthcke and D. Rowlands for helpful discussions. We would also like to thank J. Bufton for his support of our ICESat calibration

and validation efforts as part of the ICESat team, and J. Sauber for helpful editorial comments.

References

Abshire, J.B., X. Sun, H. Riris, J.M. Sirota, J.F. McGarry, S. Palm, D. Yi, and P. Liva, 2005. Geoscience Laser Altimeter System (GLAS) on the ICESat Mission: On-orbit measurement performance, *Geophysical Research Letters*, 32, L21S02, doi:10.1029/2005GL024028.

Brenner A.C., H.J. Zwally, C.R. Bentley, B.M. Csatho, D.J. Harding, M.A. Hofton, J.B. Minster, L. Roberts, J.L. Saba, R.H. Thomas, and D. Yi, 2003. Derivation of Range and Range Distributions From Laser Pulse Waveform Analysis for Surface Elevations, Roughness, Slope, and Vegetation Heights, Geoscience Laser Altimeter System Algorithm Theoretical Basis Document, Version 4.1, URL: http://www.csr.utexas.edu/glas/atbd.html (last date accesed: 12 December 2005).

Carabajal, C.C., and D.J. Harding, 2005. ICESat validation of SRTM C-band digital elevation models, *Geophysical Research Letters*, 32, L22S01, doi:10.1029/2005GL023957.

Duda, D.P., J.D. Spinhirne, and E.W. Eloranta, 2001. Atmospheric multiple scattering effects on GLAS altimetry – Part I: Calculations of single pulse bias, *IEEE Transactions on Geoscience and Remote Sensing*, 39(1):92–101.

Farr, T.G., and M. Kobrick, 2000. Shuttle Radar Topography Mission produces a wealth of data, *AGU EOS*, 81:583–585.

Fricker, H.A., A. Borsa, B. Minster, C. Carabajal, K. Quinn, and B. Bills, 2005. Assessment of ICESat performance at the salar de Uyuni, Bolivia, *Geophysical Research Letters*, 32, L21S06, doi:10.1029/2005GL023423.

Hansen, M.C., R.S. DeFries, J.R.G. Townshend, M. Carroll, C. Dimiceli, and R.A. Sohlberg, 2003. Global percent tree cover at a spatial resolution of 500 meters: First results of the MODIS vegetation continuous fields algorithm, *Earth Interactions*, 7(10):1–15.

Harding, D.J., and C.C. Carabajal, 2005. ICESat waveform measurements of within-footprint topographic relief and vegetation vertical structure, *Geophysical Research Letters*, 32, L21S10, doi:10.1029/2005GL023471.

Lemoine, F.G., S.C. Kenyon, J.K. Factor, R.G. Trimmer, N.K. Pavlis, D.S. Chinn, C.M. Cox, S.M. Klosko, S.B. Luthcke, M.H. Torrence, Y.M. Wang, R.G. Williamson, E.C. Pavlis, R.H. Rapp and T.R. Olson, 1998. *The Development of the Joint NASA GSFC and NIMA Geopotential Model EGM96*, NASA/GSFC, Greenbelt, Maryland, 575 p.

Luthcke, S., D. Rowlands, J. McCarthy, D. Pavlis and E. Stoneking, 2000. Spaceborne laser-altimeter-pointing bias calibration from range residual analysis, *Journal of Spacecraft and Rockets*, 37(3):374–384.

NGA, 1994. Military Standard World Geodetic System 84 (WGS84), URL: http://earth-info.nga.mil/GranG/wgs84/ (last date accessed: 12 December 2005).

Rabus, B., M. Eineder, A. Roth, and R. Bamler, 2003. The Shuttle Radar Topography Mission- A new class of digital elevation models acquired by spaceborne radar, *Photogrammetric Engineering & Remote Sensing*, 57:241–262.

Rodriguez, E., C.S. Morris, J.E. Belz, E.C. Chapin, J.M. Martin, W. Daffer and S. Hensley, 2005. *An Assessment of the SRTM Topographic Products*, NASA Jet Propulsion Laboratory, D-31639.

Schutz, B., H.J. Zwally, C.A. Shuman, D. Hancock, and J.P. DiMarzio, 2005. Overview of the ICESat mission, *Geophysical Research Letters*, 32, L21S01, doi:10.1029/2005GL024009.

Spinhirne, J.D., S.P. Palm, W.D. Hart, D.L. Hlavka, and E.J. Welton, 2005. Cloud and aerosol measurements from GLAS: Overview and initial results, *Geophysical Research Letters*, 32, L22S03, doi:10.1029/2005GL023507.

Zwally, H.J., B. Schutz, W. Abdalati, J. Abshire, C. Bentley, A. Brenner, J. Bufton, J. Dezio, D. Hancock, D. Harding, T. Herring, B. Minster, K. Quinn, S. Palm, J. Spinhirne, and R. Thomas, 2002. ICESat's laser measurements of polar ice, atmosphere, ocean and land, *Journal of Geodynamics*, 34:405–445.